Original Article

# The role of lumbosacral paraspinal muscle degeneration and low vertebral bone mineral density on distal instrumentation-related problems following long-instrumented spinal fusion for degenerative lumbar scoliosis: a retrospective cohort study

**Honghao Yang[#]^, Zhangfu Li[#], Yong Hai^, Hanwen Zhang**

Department of Orthopedic Surgery, Beijing Chao-Yang Hospital, Beijing, China

*Contributions:* (I) Conception and design: Y Hai; (II) Administrative support: Y Hai; (III) Provision of study materials or patients: Y Hai, H Zhang; (IV) Collection and assembly of data: H Yang, Z Li; (V) Data analysis and interpretation: H Yang, Z Li, H Zhang; (VI) Manuscript writing: All authors; (VII) Final approval of manuscript: All authors.

[#]These authors contributed equally to this work and should be considered as co-first authors.

*Correspondence to:* Yong Hai, MD, PhD. Department of Orthopedic Surgery, Beijing Chao-Yang Hospital, Capital Medical University, Gongti South Rd., No. 8, Beijing 100020, China. Email: spinesurgeon@ccmu.edu.cn.

**Background:** This study aimed to confirm the role of paraspinal muscle degeneration and low vertebral bone mineral density (vBMD) of the lumbosacral region in the development of distal instrumentation-related problems (DIPs) in degenerative lumbar scoliosis (DLS) patients undergoing long-instrumented spinal fusion.

**Methods:** From 2013 to 2019, 125 DLS patients with 24-month follow-up after long-instrumented spinal fusion in Beijing Chao-Yang Hospital were retrospectively recruited and divided into DIP and non-DIP groups. Demographic characteristics, surgical data, and radiographic parameters were statistically compared between the groups. Degeneration of the paraspinal muscle was evaluated using the relative gross cross-sectional area (rGCSA), relative functional cross-sectional area (rFCSA), ratio of the rFCSA to rGCSA, gross muscle-fat index, and functional muscle-fat index of the multifidus (MF), erector spinae (ES), paraspinal extensor muscle (PSE), and psoas major determined by preoperative magnetic resonance imaging (MRI). The vBMD of the lumbosacral region and lower instrumented vertebra (LIV) was assessed using Hounsfield unit (HU) values determined by computed tomography (CT) scans. The DeLong test was performed to select MRI and CT scan variables. Multivariable logistic regression analysis was applied to determine the independent predictive factors of DIPs.

**Results:** The incidence of DIPs was 16.0% (20/105). There were no significant differences in demographic characteristics or surgical data between the groups. The rFCSAs of the MF (65.74±21.51 *vs.* 92.37±21.68; P<0.001), ES (82.67±21.44 *vs.* 111.48±24.21; P<0.001) and PSE (144.31±36.12 *vs.* 208.48±41.57; P<0.001) and the HU values of the lumbosacral region (103.80±22.64 *vs.*. 132.19±19.17; P<0.001) and LIV (111.70±23.23 *vs.* 128.69±20.70; P=0.005) were significantly lower in the DIP group. Significantly less preoperative pelvic tilt and greater postoperative lumbosacral lordosis and sagittal vertical axis (SVA) values were observed in the DIP group. The rFCSA of the PSE, the HU value of the lumbosacral region, and the postoperative SVA value were detected as independent predictive factors of DIPs.

^ ORCID: Yong Hai, 0000-0002-7206-325X; Honghao Yang, 0000-0001-5300-1283.

**Conclusions:** Lower muscularity of the PSE, a lower vBMD of the lumbosacral region, and postoperative sagittal malalignment were independent predictive factors of DIPs. Surgeons should emphasize the preoperative evaluation of paraspinal muscle and bone mass in DLS patients.

**Keywords:** Lumbosacral paraspinal muscle degeneration; fatty infiltration; low vertebral bone mineral density; degenerative lumbar scoliosis; distal instrumentation-related problems

Submitted Dec 15, 2022. Accepted for publication Apr 21, 2023. Published online May 15, 2023.
doi: 10.21037/qims-22-1394
**View this article at:** https://dx.doi.org/10.21037/qims-22-1394

## Introduction

Degenerative lumbar scoliosis (DLS) is a kind of adult spinal deformity defined as a lumbar Cobb angle greater than 10° (1,2). The prevalence of DLS ranges from 7.5% to 68.0% worldwide and continues to increase with the aging of the population (3). Severe low back and leg pain could be caused by lateral olisthesis-induced or rotatory subluxation-induced foraminal stenosis, persistently impacting patients' daily activities (4-7). If relief is not achieved with conservative treatment, decompression and restoration of spinal alignment by long-instrumented spinal fusion can be considered.

A high complication rate of long-instrumented spinal fusion for DLS has been reported, and the most common complication is related to instrumentation, with an incidence ranging from 12.4% to 31.7% (8-10). Distal instrumentation-related problems (DIPs) are a series of complications related to the lower instrumented vertebra (LIV), including distal junctional kyphosis (11), screw loosening or breakage (12), fracture of the LIV (13), and segmental instability (14), which can significantly impact postoperative health-related quality of life (HRQoL) (15). For patients with severe neurological symptoms caused by DIPs, revision surgery may be needed. The development of DIPs is multifactorial, and various predictive factors of DIPs have been reported, including age, preoperative sagittal malalignment, high body mass index (BMI), and LIV selection (11,16).

Recently, the role of paraspinal muscle degeneration and low vertebral bone mineral density (vBMD), evaluated by Hounsfield unit (HU) values determined by computed tomography (CT) scans, has been increasingly investigated in patients with DLS (3,17-21). A lower muscularity of the paraspinal muscle is associated with persistent low back pain, the loss of lumbar lordosis, disability, and proximal junctional mechanical complications (22,23). Lower HU values of the vertebral body and pedicle trajectory could induce a high risk of stress fracture and implant failure in patients who undergo lumbar fusion (24). However, the effect of muscularity and the vBMD of the lumbosacral region on the development of DIPs in patients with DLS is still unknown.

This study aimed to confirm the relationship among paraspinal muscle degeneration, a low vBMD of the lumbosacral region, and DIPs in patients who undergo long-instrumented spinal fusion for DLS. We present this article in accordance with the STROBE reporting checklist (available at https://qims.amegroups.com/article/view/10.21037/qims-22-1394/rc).

## Methods

### *Study design and participants*

This was a single-center retrospective cohort study. The study was conducted in accordance with the Declaration of Helsinki (as revised in 2013). The study was approved by the Research Ethics Committee of Beijing Chao-Yang Hospital (No. 2021-09-07-10), and the need for individual consent for this retrospective analysis was waived. From January 2013 to December 2019, patients who underwent posterior instrumentation and fusion for DLS with a minimum 24-month follow-up in Beijing Chao-Yang Hospital were retrospectively recruited. The follow-up procedures included physical examinations and standing full-length spine radiographs at 3, 6, 12, and 24 months postoperatively. The inclusion criteria were as follows: (I) an age >50 years old at the time of surgery; (II) a Cobb angle of scoliosis >10°; (III) instrumented levels ≥4; (IV) LIV at or above S1; (V) upper instrumented vertebra (UIV) at or above L2; and (VI) a duration of follow-up ≥24 months. Patients with other etiologies of spinal deformity, tumors, infections, a history of spinal surgery, and nonambulatory status were excluded from this study. In our hospital, spinopelvic fixation is not routinely performed in DLS patients. Considering that the placement of pelvic screws would significantly influence the biomechanical characteristics of the spine and that extensive dissection would directly reduce the function of the paraspinal muscle, to eliminate the impact of these factors on the outcomes, patients undergoing spinopelvic fixation were also excluded. Patients with a concomitant diagnosis of osteoporosis began antiosteoporosis therapy after discharge from the hospital.

### *Diagnostic criteria of distal instrumentation-related problems*

The included patients were divided into two groups based on the occurrence of DIPs during the follow-up period. The diagnostic criteria for DIPs were as follows: (I) distal junctional kyphosis, which indicated that the distal junctional angle (formed by the superior endplate of the LIV and the inferior endplate of the adjacent distal vertebra) was at least 10° at the last follow-up and at least 10° greater than the preoperative measurement; (II) screw loosening, pull-out, or breakage at the LIV; (III) fracture of the LIV; (IV) segmental instability at the distal level of the LIV; and (V) the requirement for revision surgery due to severe clinical symptoms caused by instrument failure of the LIV (16,25). Patients who met one of the above diagnostic criteria were classified into the DIP group; otherwise, they were included in the non-DIP group.

### *Data collection*

Demographic information was collected, including sex, age, BMI, and comorbidities. Surgical data, including the location of the UIV and LIV, levels of instrumentation, levels of interbody fusion, osteotomy status, rod material, and rod diameters, were recorded. For patients with LIV at S1, the performance of L5-S1 interbody fusion was also recorded. Full-length spine standing radiographs were obtained preoperatively and ≤2 weeks postoperatively. Radiographic parameters, including Cobb angle values, lumbar lordosis (LL, L1–S1), lumbosacral lordosis (LSL, L4-S1), sagittal vertical axis (SVA), T1 pelvic angle (TPA), pelvic tilt (PT), sacral slope (SS), pelvic incidence (PI), and incidence of PI-LL mismatch, were measured by two senior spinal surgeons with the Picture Archiving and Communication System (PACS). PI-LL mismatch indicated that the absolute value of PI minus LL was greater than 10°. Two spine surgeons independently collected these data from April 2022 to September 2022.

### *Paraspinal muscle evaluation by magnetic resonance imaging*

Preoperative magnetic resonance imaging (MRI) of the lumbar spine was performed using Signa HDxt 3.0 T (General Electric Company), with a slice thickness of 3 mm. The slicing plane was parallel to the inferior endplate of the vertebral body. Axial T2-weighted images at the inferior vertebral endplate level of L4 and L5 were exported as Digital Imaging and Communications in Medicine (DICOM) data and analyzed using ImageJ software 1.52k (National Institutes of Health, USA).

The mean values of the cross-sectional area (CSA) and signal intensity (SI) of the multifidus (MF), erector spinae (ES), paraspinal extensor muscle (PSE), and psoas major (PS) were measured (*Figure 1A*,*1B*). The PSE indicated the combination of the MF and ES. The mean values of both the CSA and SI at L4 and L5 were calculated to reflect the muscularity and fatty infiltration of the paraspinal muscle at the lumbosacral region. To decrease the bias caused by patient stature, the relative cross-sectional area (rCSA), which indicated the ratio of the CSA of the muscle to that of the vertebral body, was applied. The gross cross-sectional area (GCSA) included the CSA of lean muscle, intramuscular fat, and soft tissue, while the functional cross-sectional area (FCSA) solely indicated the CSA of lean muscle (3). Then, the relative gross cross-sectional area (rGCSA) and relative functional cross-sectional area (rFCSA) were calculated, and their values were multiplied by 100 and used for statistical analysis (20). The ratio of the rFCSA to the rGCSA (F/G ratio) was also calculated. The muscle-fat index (MFI) indicated the ratio of the SI of muscle to that of subcutaneous fat (26). The MFIs of gross and functional muscle were defined as the gross MFI (GMFI) and functional MFI (FMFI), respectively.

### *Vertebral bone mineral density evaluation by CT scan*

Preoperative lumbar spine CT scans were performed in the supine position with the following parameters: 320 mAs, 120 kVP, and a 5-mm thickness. The slicing plane was parallel to the endplates of the vertebral body on the coronal and sagittal planes, through the midpoint of the posterior edge of the spinal canal and the anterior edge of the vertebral body on the axial plane. Four images were obtained for each

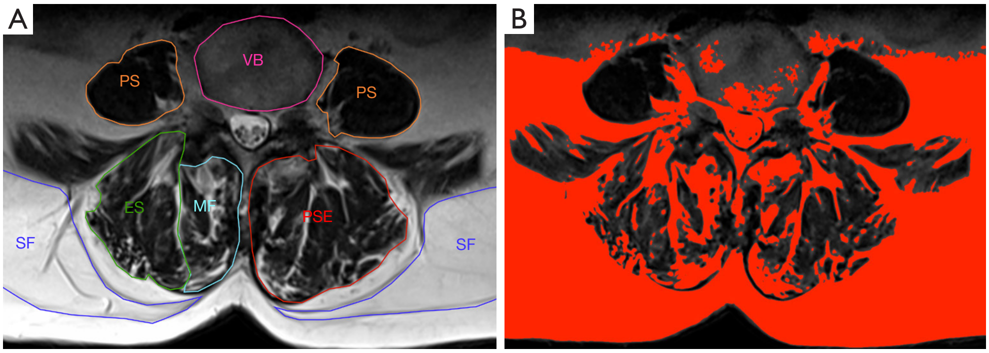


**Figure 1** Measurement of paraspinal muscle parameters. (A) Preoperative lumbar spine magnetic resonance imaging; (B) ImageJ software. The red region indicates intramuscular fat, soft tissue, and subcutaneous fat through the threshold technique. MF, multifidus; ES, erector spinae; PSE, paraspinal extensor muscle; PS, psoas major; VB, vertebral body; SF, subcutaneous fat.

vertebra: for L4 and L5, the sagittal image at the midsagittal plane and three axial images (immediately inferior to the superior endplate, in the middle of the vertebral body, and immediately superior to the inferior endplate) were selected (21); for S1, the sagittal image at the midsagittal plane and three consecutive axial images immediately inferior to the superior endplate were selected (27). The region of interest (ROI) on each image was circular or oval and as large as possible, excluding the cortical margins, osteosclerotic areas, and osteophytes to prevent volume averaging (*Figure 2A-2F*). The HU value of each ROI was measured using OsiriX 13.0.1 software (Pixmeo Sarl, Switzerland). The mean HU value of the four ROIs was calculated as the HU value of the vertebral body. Then, the mean HU values of L4, L5, and S1 were calculated to reflect the vBMD of the lumbosacral region. The HU value of the LIV was also measured. The relationship between the HU values and dual-energy X-ray absorptiometry (DXA)-assessed BMD was evaluated by Pearson correlation analysis.

It should be noted that the imaging examinations were performed by the radiologic technologists who were duty that day. They all received the same training and obtained the same qualifications and certificates, and their operations were consistent. The radiologic technologists were blinded to the grouping of the patients and the grouping information of the MRI and CT images.

### *Statistical analysis*

All statistical analyses were performed utilizing SPSS 25.0 (Chicago, IL, USA) and MedCalc 19.1.3 (Ostend, Belgium). A two-sided P value of less than 0.05 was considered statistically significant. The Shapiro-Wilk test was performed to determine whether continuous variables had a normal distribution. Continuous variables with a normal distribution are presented as the mean ± standard deviation; otherwise, the median and interquartile range are used. The counts and percentages are presented for categorical variables. For the comparison of continuous variables between the DIP and non-DIP groups, the independent-sample *t*-test or nonparametric Mann-Whitney U test was performed; for categorical variables, the Pearson chi-square test or Fisher's exact test was applied. Since all the patients included in this study were from our hospital, their data were available in our quality-controlled medical record system and the PACS. Therefore, there were no missing data.

The receiver operating characteristic curve was constructed using each MRI and CT scan parameter, and the best cutoff value was determined. The area under the curve (AUC) of each parameter was calculated. For each MRI parameter of each muscle, the variable with the maximum AUC was selected for the subsequent analysis. Then, the DeLong test was applied to select the MRI parameter and CT scan parameter with the most discriminatory ability for predicting DIPs.

Logistic regression analysis was performed to explore the potential predictive factors of DIPs. Demographic, radiographic, and surgical variables were first selected using univariate analysis. Significant factors and previously selected MRI/CT scan parameters were included in the multivariable logistic regression analysis to determine the independent predictive factors of DIPs. The odds ratio (OR) and 95% confidence interval (CI) were used.

 

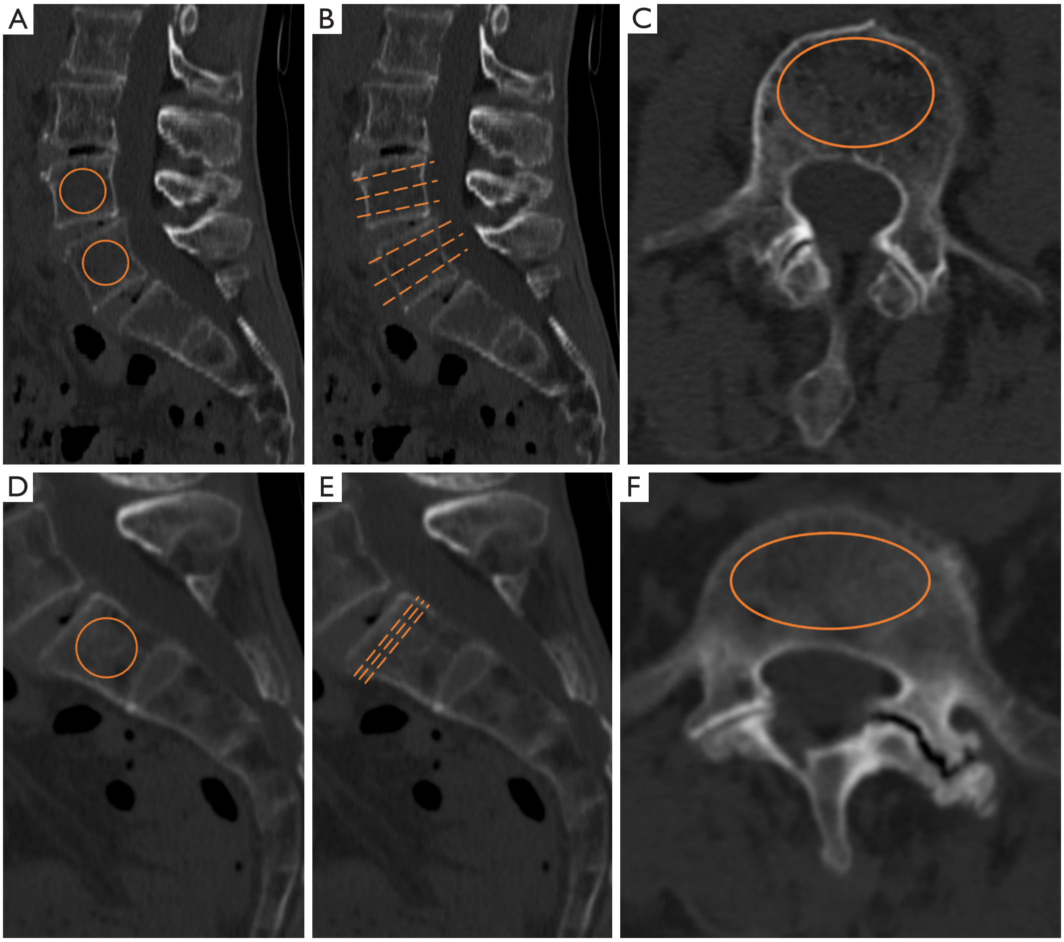


**Figure 2** Measurement of HU values on a preoperative lumbar spine CT scan. The orange lines indicate the slicing planes. The orange circles indicate the ROI. (A) The ROI at the midsagittal plane image for L4 and L5; (B) The slicing planes at the midsagittal plane for L4 and L5; (C) The ROI at the axial plane image for L4 and L5; (D) The ROI at the midsagittal plane image for S1; (E) The slicing planes at the midsagittal plane for S1; (F) The ROI at the axial plane image for S1. ROI, region of interest; HU, Hounsfield unit.

## Results

### *Demographic characteristics and surgical data*

One hundred fifty-seven patients were screened, and 125 patients (70 females, 55 males) who met the inclusion and exclusion criteria were recruited for this study (*Figure 3*). The mean age at surgery was 66.57±5.92 years, and the mean duration of follow-up was 27.23±3.32 months. The incidence of DIPs was 16.0% (20/125). The demographic information and surgical data are summarized in *Table 1*. There were no significant differences in age (P=0.71), BMI (P=0.71), hypertension (P=0.21), chronic obstructive pulmonary disease (P=0.51), coronary artery disease (P=0.63), diabetes mellitus (P=0.22), the UIV (P=0.73) and LIV locations (P=0.54), the levels of instrumentation (P=0.23), the levels of interbody fusion (P=0.83), the performance of L5-S1 interbody fusion (for patients with LIV at S1) (P=0.89), osteotomy status (P=0.37), the rod material (P=0.64), or the rod diameter (P=0.30) between the DIP and the non-DIP groups. There were no patients who underwent three-column osteotomy (3-CO). As multiple-rod constructs were not routinely performed for DLS patients before June 2021 in our hospital, two-rod constructs were used for all recruited patients in the current study.

### *Degeneration of the paraspinal muscle of the lumbosacral region by MRI parameters*

There was no significant difference in the rGCSA of each

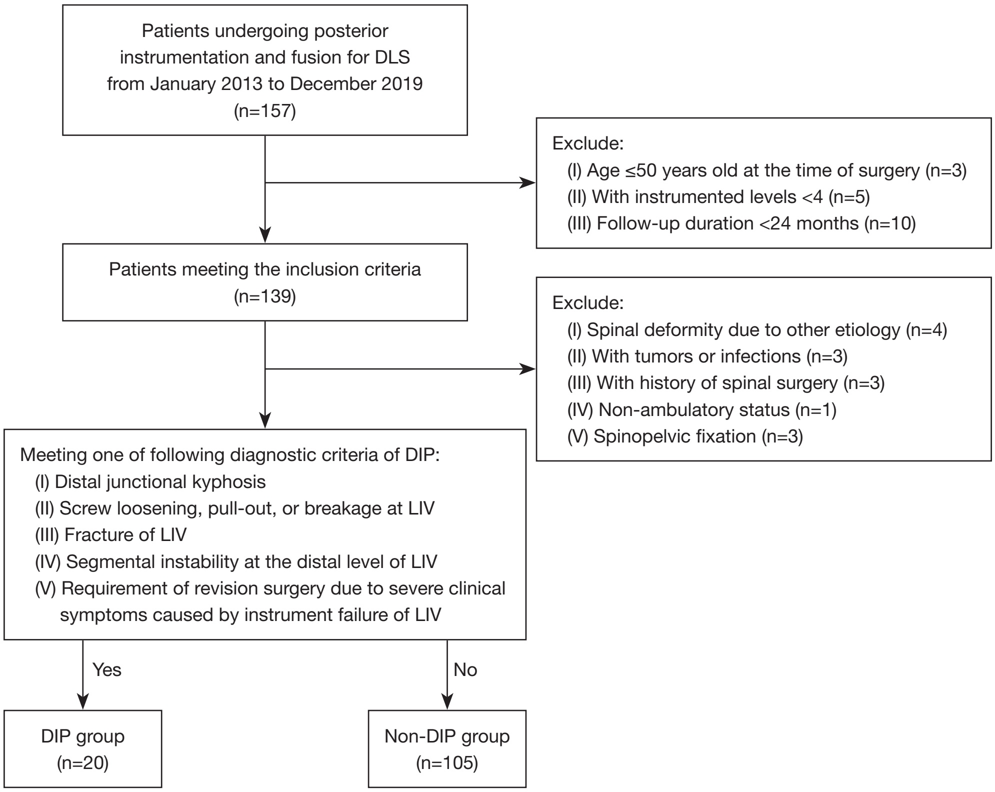


**Figure 3** Flow chart of patient inclusion and exclusion. DLS, degenerative lumbar scoliosis; DIPs, distal instrumentation-related problems; LIV, lower instrumented vertebra.

muscle between the DIP and non-DIP groups. Additionally, none of the MRI parameters of the PS were significantly different between the groups. However, the rFCSA and F/G ratio of the MF, ES, and PSE were significantly smaller or lower, while the GMFI and FMFI were significantly greater in the DIP group (*Table 2* and *Figure 4A-4E*). Among the MRI parameters, the maximum AUC was observed in the rGCSA for the ES (0.528), rFCSA for the PSE (0.917), F/G ratio for the PSE (0.833), GMFI for the MF (0.784), and FMFI for the MF (0.805) (*Figure 5A-5E*). The DeLong test revealed that the AUC of the rFCSA for the PSE was significantly greater than that of the other four parameters (*Figure 6*). The cutoff value was 154.26, with a sensitivity and specificity of 88.6% and 85.0%, respectively.

### *Vertebral bone mineral density of the lumbosacral region by CT scan parameters*

The HU value of the lumbosacral region (103.80±22.64 *vs.* 132.19±19.17; 95% CI: −37.064 to −19.717; P<0.001) and LIV (111.70±23.23 *vs.* 128.69±20.70; 95% CI: −32.154 to −8.583; P=0.005) were significantly lower in the DIP group than in the non-DIP group (*Table 3*). The Pearson correlation analysis revealed a significantly positive relationship between DXA-assessed BMD and the HU value of the lumbosacral region (r=0.832, P<0.001) or the HU value of the LIV (r=0.745, P=0.005). According to the DXA outcome, the incidence of osteoporosis was significantly higher in the DIP group than in the non-DIP group (85.0% *vs.* 61.0%, P=0.04). The DeLong test revealed that the AUC of the HU value of the lumbosacral region was significantly greater than that of the LIV (0.858 *vs.* 0.756; 95% CI: 0.016 to 0.204; P=0.04), with cutoff values of 112.03 and 101.39, respectively.

### *Radiographic parameters*

There were no significant differences between the groups in the preoperative Cobb angle, LL, LSL, SVA, TPA, or SS. However, the preoperative PT was significantly lower in the DIP group than in the non-DIP group (19.86±9.33 *vs.* 24.56±9.54; 95% CI: 0.056 to 9.358; P=0.05). For

**Table 1** Comparison of demographic information and surgical data between the DIP and non-DIP groups

| Variable | DIP group (n=20) | Non-DIP group (n=105) | 95% CI | P value |
|---|---|---|---|---|
| Demographic Information | | | | |
| Age (years) | 66.20±6.71 | 66.74±5.79 | −2.327 to 3.413 | 0.71 |
| Sex | | | | 0.38 |
| Male | 7 (35.0) | 48 (45.7) | | |
| Female | 13 (65.0) | 57 (54.3) | | |
| BMI (kg/m$^2$) | 25.82±2.88 | 25.57±2.17 | −1.655 to 1.146 | 0.71 |
| Comorbidities | | | | |
| Hypertension | 9 (45.0) | 63 (60.0) | | 0.21 |
| COPD | 4 (20.0) | 15 (14.3) | | 0.51 |
| CAD | 7 (35.0) | 31 (29.5) | | 0.63 |
| Diabetes mellitus | 2 (10.0) | 23 (21.9) | | 0.22 |
| Surgical Data | | | | |
| Location of the UIV | | | | 0.73 |
| At L2 | 11 (55.0) | 67 (63.8) | | |
| Between T11 and L1 | 2 (10.0) | 7 (6.7) | | |
| Above/at T10 | 7 (35.0) | 31 (29.5) | | |
| Location of the LIV | | | | 0.54 |
| Above/at L5 | 14 (70.0) | 66 (62.9) | | |
| At S1 | 6 (30.0) | 39 (37.1) | | |
| Level of instrumentation | 5.75±1.98 | 5.43±1.95 | −1.471 to 0.628 | 0.23 |
| Interbody fusion | | | | 0.62 |
| No | 6 (30.0) | 26 (24.8) | | |
| Yes | 14 (70.0) | 79 (75.2) | | |
| Level of interbody fusion | 1.95±1.19 | 2.06±1.04 | −0.459 to 0.569 | 0.83 |
| Osteotomy status | | | | 0.37 |
| No | 14 (70.0) | 83 (79.0) | | |
| Yes | 6 (30.0) | 22 (21.0) | | |
| Rod material | | | | 0.64 |
| Titanium alloy | 18 (90.0) | 98 (93.3) | | |
| Cobalt chrome | 2 (10.0) | 7 (6.7) | | |
| Rod diameter | | | | 0.30 |
| 5.5 mm | 12 (60.0) | 75 (71.4) | | |
| 6.0 mm | 8 (40.0) | 30 (28.6) | | |

Data are presented as mean ± standard deviation or n (%). BMI, body mass index; UIV, upper instrumented vertebra; LIV, lower instrumented vertebra; DIPs, distal instrumentation-related problems; COPD, chronic obstructive pulmonary disease; CAD, coronary artery disease; CI, confidence interval.

**Table 2** Comparison of paraspinal muscle degeneration of the lumbosacral region between groups and the AUC of each parameter

| Variable | DIP group (n=20) | Non-DIP group (n=105) | [1]95% CI | [1]P value | AUC | [2]95% CI | [2]P value |
|---|---|---|---|---|---|---|---|
| rGCSA | | | | | | | |
| MF | 125.17±26.58 | 124.45±25.77 | −12.549 to 11.979 | 0.96 | 0.507 | 0.367 to 0.646 | >0.99 |
| ES | 152.30±27.53 | 155.21±29.63 | −17.895 to 12.081 | 0.70 | 0.528 | 0.395 to 0.661 | 0.69 |
| PSE | 272.32±49.09 | 283.67±48.78 | −26.771 to 20.387 | 0.79 | 0.511 | 0.378 to 0.644 | 0.87 |
| PS | 146.52±30.36 | 151.11±33.27 | −21.573 to 12.395 | 0.59 | 0.510 | 0.382 to 0.637 | 0.89 |
| rFCSA | | | | | | | |
| MF | 65.74±21.51 | 92.37±21.68 | −37.091 to −16.177 | <0.001 | 0.823 | 0.710 to 0.936 | <0.001 |
| ES | 82.67±21.44 | 111.48±24.21 | −39.734 to −17.869 | <0.001 | 0.827 | 0.721 to 0.934 | <0.001 |
| PSE | 144.31±36.12 | 208.48±41.57 | −82.807 to −57.453 | <0.001 | 0.917 | 0.865 to 0.968 | <0.001 |
| PS | 122.86±26.78 | 129.30±29.84 | −21.762 to 8.885 | 0.41 | 0.519 | 0.394 to 0.643 | 0.79 |
| F/G ratio | | | | | | | |
| MF | 0.55±0.13 | 0.72±0.10 | −0.188 to −0.041 | 0.004 | 0.773 | 0.653 to 0.893 | <0.001 |
| ES | 0.56±0.14 | 0.70±0.11 | −0.219 to −0.112 | 0.002 | 0.751 | 0.614 to 0.888 | <0.001 |
| PSE | 0.56±0.15 | 0.75±0.12 | −0.232 to −0.134 | <0.001 | 0.833 | 0.710 to 0.955 | <0.001 |
| PS | 0.83±0.05 | 0.87±0.04 | −0.034 to 0.003 | 0.11 | 0.635 | 0.507 to 0.762 | 0.06 |
| GMFI | | | | | | | |
| MF | 0.50±0.16 | 0.35±0.13 | 0.091 to 0.220 | <0.001 | 0.784 | 0.671 to 0.898 | <0.001 |
| ES | 0.48±0.18 | 0.31±0.14 | 0.096 to 0.235 | 0.002 | 0.760 | 0.633 to 0.886 | <0.001 |
| PSE | 0.51±0.21 | 0.34±0.11 | 0.107 to 0.241 | 0.002 | 0.732 | 0.583 to 0.881 | 0.001 |
| PS | 0.16±0.04 | 0.15±0.04 | −0.009 to 0.029 | 0.29 | 0.588 | 0.447 to 0.730 | 0.21 |
| FMFI | | | | | | | |
| MF | 0.33±0.11 | 0.22±0.08 | 0.067 to 0.150 | <0.001 | 0.805 | 0.696 to 0.914 | <0.001 |
| ES | 0.35±0.13 | 0.23±0.10 | 0.076 to 0.177 | <0.001 | 0.797 | 0.680 to 0.915 | <0.001 |
| PSE | 0.34±0.12 | 0.21±0.08 | 0.086 to 0.168 | <0.001 | 0.788 | 0.652 to 0.925 | <0.001 |
| PS | 0.12±0.02 | 0.11±0.03 | −0.002 to 0.024 | 0.10 | 0.625 | 0.493 to 0.757 | 0.08 |

Data are presented as mean ± standard deviation. [1], independent-sample *t*-test; [2], receiver operating characteristic curve analysis. rGCSA, relative gross cross-sectional area; rFCSA, relative functional cross-sectional area; F/G ratio, the ratio of the rFCSA to the rGCSA; GMFI, gross muscle-fat index; FMFI, functional muscle-fat index; MF, multifidus; ES, erector spinae; PSE, paraspinal extensor muscle; PS, psoas major; AUC, area under the curve; DIPs, distal instrumentation-related problems; CI, confidence interval.

postoperative radiographic parameters, there were no significant differences in the Cobb angle, LL, TPA, PT, SS, PI-LL, or the incidence of PI-LL mismatch between the groups. The postoperative LSL (33.63±9.58 *vs.* 28.48±9.41; 95% CI: −9.705 to −0.591; P=0.03) and SVA [38.84±17.83 *vs.* 25.30 (12.00, 33.27), P<0.001] were significantly greater in the DIP group than in the non-DIP group (*Table 4*). No significant difference in PI was detected between the groups (47.06±8.50 *vs.* 48.47±11.40; 95% CI: −3.903 to 6.722; P=0.60). According to the above results, the preoperative PT, postoperative LSL, and postoperative SVA were selected for further multivariable logistic regression analysis.

### *Independent predictive factors of DIPs by multivariable logistic regression analysis*

Based on the results of the previous analysis, the preoperative PT, the postoperative LSL, the postoperative

 

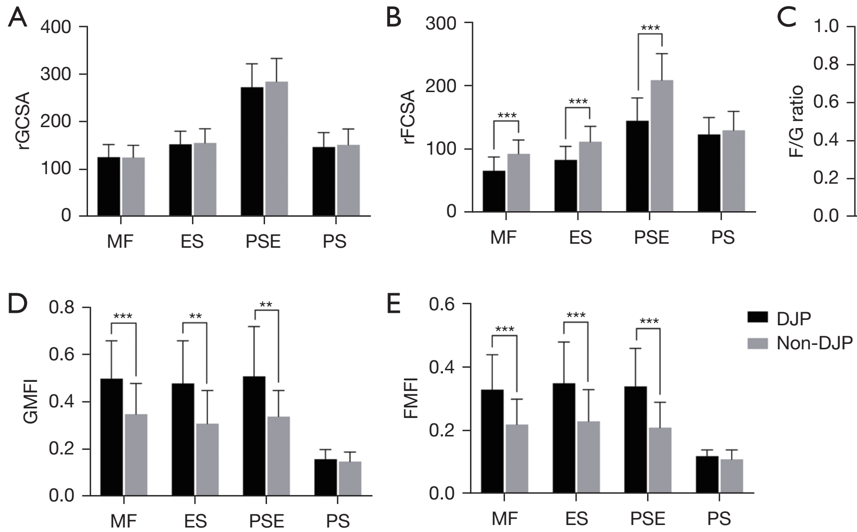


**Figure 4** Differences in the rGCSA, rFCSA, F/G ratio, GMFI and FMFI of each muscle regarding the development of DIPs. (A) rGCSA; (B) rFCSA; (C) F/G ratio; (D) GMFI; (E) FMFI. **, P<0.01; ***, P<0.001; rGCSA, relative gross cross-sectional area; rFCSA, relative functional cross-sectional area; F/G ratio, the ratio of the rFCSA to the rGCSA; GMFI, gross muscle-fat index; FMFI, functional muscle-fat index; DIPs, distal instrumentation-related problems; MF, multifidus; ES, erector spinae; PSE, paraspinal extensor muscle; PS, psoas major.

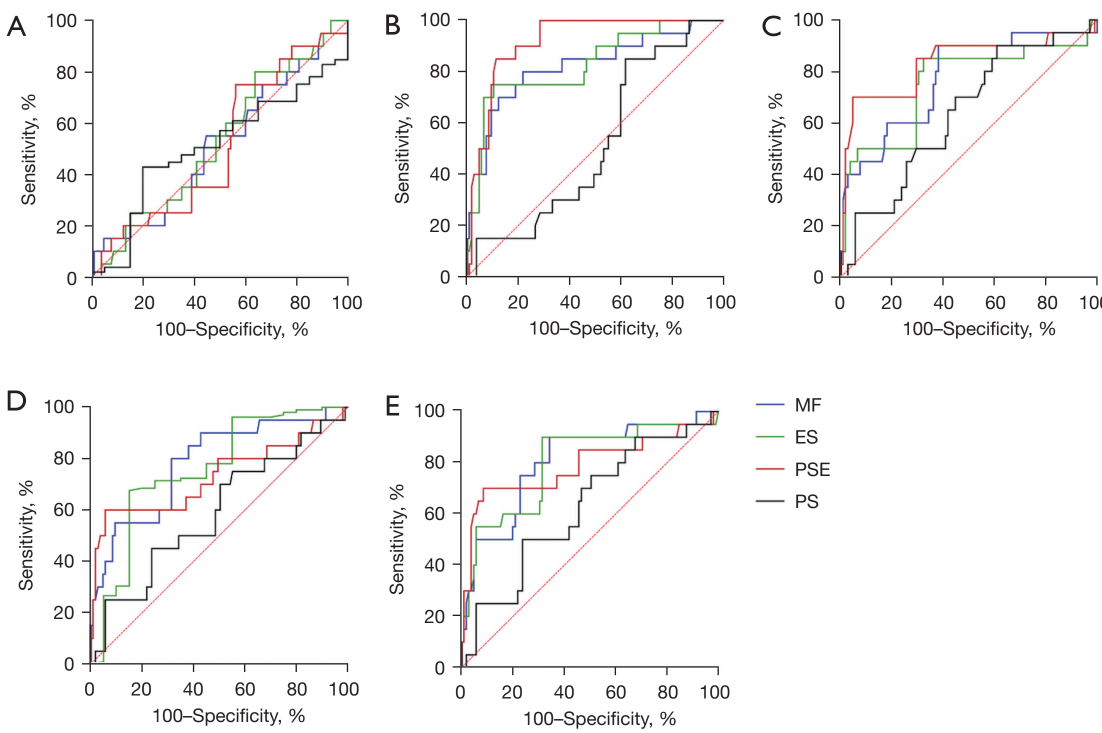


**Figure 5** The ROC of the rGCSA, rFCSA, F/G ratio, GMFI and FMFI of each muscle. (A) rGCSA; (B) rFCSA; (C) F/G ratio; (D) GMFI; (E) FMFI. rGCSA, relative gross cross-sectional area; rFCSA, relative functional cross-sectional area; F/G ratio, the ratio of the rFCSA to the rGCSA; GMFI, gross muscle-fat index; FMFI, functional muscle-fat index; ROC, receiver operating characteristic; MF, multifidus; ES, erector spinae; PSE, paraspinal extensor muscle; PS, psoas major.

 

SVA, the rFCSA of the PSE, and the HU value of the lumbosacral region remained as covariates for inclusion in multivariable logistic regression analysis. In the multivariable model, the rFCSA of the PSE (OR 0.958; 95% CI: 0.936 to 0.981, P<0.001), the HU value of the lumbosacral region (OR 0.941; 95% CI: 0.906 to 0.977, P=0.002), and the postoperative SVA (OR 1.047; 95% CI: 1.003 to 1.093, P=0.04) were detected as independent predictive factors of DIPs (*Table 5*). An illustrative case is demonstrated in *Figure 7A-7S*.

## Discussion

Owing to the accumulating evidence indicating that the restoration of spinal alignment could better improve HRQoL for DLS patients, an increasing number of long-instrumented spinal fusions have been performed in recent decades (28-30). Proximal junctional kyphosis/failure, which is a common mechanical complication that occurs at the proximal end of instrumentation, has been widely reported by previous studies (31-33). Low muscularity and vBMD at the UIV have been identified as predictive factors for this complication (21,34). Similarly, DIPs include mechanical complications at the distal end of instrumentation, which could cause sagittal decompensation, neurological symptoms and revision requirements, having a devastating impact on patients' HRQoL (13,35). However, studies focused on DIPs in DLS patients are still limited, and the role of paraspinal muscle degeneration and a low vBMD of the lumbosacral region is poorly understood. The current study observed DIPs in 20 patients, with an incidence of 16.0%. We found that a preoperative low lean muscle mass, a low vBMD, and postoperative sagittal malalignment could independently increase the risk of DIPs in DLS patients after long-instrumented spinal fusion.

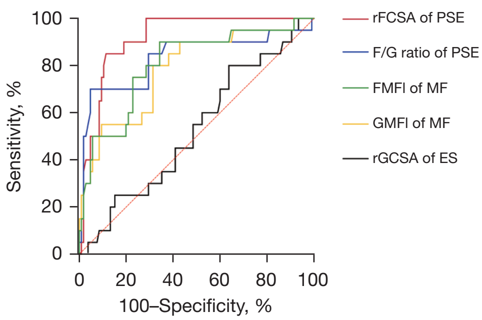


**Figure 6** Results of the DeLong test. rGCSA, relative gross cross-sectional area; rFCSA, relative functional cross-sectional area; F/G ratio, the ratio of the rFCSA to the rGCSA; GMFI, gross muscle-fat index; FMFI, functional muscle-fat index; MF, multifidus; ES, erector spinae; PSE, paraspinal extensor muscle.

The paraspinal muscle plays an important role in maintaining spinal stability and alignment (36). The paraspinal muscle of the lumbosacral region could support the spine, protecting against and distributing stress on the instrumentation. The stress on the instrumentation of the LIV is the strongest because it is located at the transition region between the instrumented and mobile spine, which has contrary biomechanical characteristics. In long-instrumented spinal fusion for DLS, the LIV is commonly at L5 or S1; however, fixation in the lumbosacral junction continues to be a challenge due to its unique biomechanical forces, anatomy, and sacral cancellous nature (37,38). The degeneration of the paraspinal muscle, which is presented as a decreasing CSA and high FI, would impact its strength and function, resulting in more biomechanical stress on the instrumentation of the LIV (39). Additionally, the extensive dissection of the PSE during surgery would increase the

**Table 3** Comparison of the vertebral bone mineral density of the lumbosacral region and LIV between the groups, the AUC of each parameter, and the outcome of DeLong test

| Variable | DIP group (n=20) | Non-DIP group (n=105) | [1]95% CI | [1]P value | AUC | [2]95% CI | [2]P value | AUC difference | [3]95% CI | [3]P value |
|---|---|---|---|---|---|---|---|---|---|---|
| HU value | | | | | | | | | | |
| Lumbosacral region | 103.80±22.64 | 132.19±19.17 | −37.064 to −19.717 | <0.001 | 0.858 | 0.749 to 0.966 | <0.001 | 0.102 | 0.016 to 0.204 | 0.04 |
| LIV | 111.70±23.23 | 128.69±20.70 | −32.154 to −8.583 | 0.005 | 0.756 | 0.641 to 0.872 | <0.001 | | | |

Data are presented as mean ± standard deviation. [1], independent-sample *t*-test; [2], receiver operating characteristic curve analysis; [3], DeLong test. HU, Hounsfield unit; LIV, lower instrumented vertebra; AUC, area under the curve; DIP, distal instrumentation-related problem; CI, confidence interval.

**Table 4** Comparison of radiographic parameters between the DIP and Non-DIP groups

| Variable | DIP group (n=20) | Non-DIP group (n=105) | 95% CI | P value |
|---|---|---|---|---|
| Cobb angle (°) | | | | |
| Preoperative | 19.07±4.53 | 21.26±5.01 | −0.990 to 5.384 | 0.18 |
| Postoperative | 8.93±4.58 | 10.06±4.92 | −2.694 to 5.555 | 0.49 |
| LL (°) | | | | |
| Preoperative | 30.84±15.78 | 29.60±14.18 | −8.205 to 5.738 | 0.73 |
| Postoperative | 45.01±14.52 | 41.42±12.70 | −9.868 to 2.688 | 0.26 |
| LSL (°) | | | | |
| Preoperative | 29.13±10.82 | 26.69±11.73 | −8.040 to 3.157 | 0.39 |
| Postoperative | 33.63±9.58 | 28.48±9.41 | −9.705 to −0.591 | 0.03 |
| SVA (°) | | | | |
| Preoperative | 47.69±21.58 | 36.65±23.99 | −22.449 to 0.377 | 0.06 |
| Postoperative | 38.84±17.83 | 25.30 (12.00, 33.27) | | <0.001 |
| TPA (°) | | | | |
| Preoperative | 20.28±10.84 | 23.27±10.22 | −1.994 to 7.971 | 0.24 |
| Postoperative | 14.94±10.04 | 18.58±9.38 | −0.943 to 8.217 | 0.12 |
| PT (°) | | | | |
| Preoperative | 19.86±9.33 | 24.56±9.54 | 0.056 to 9.358 | 0.05 |
| Postoperative | 22.91±8.84 | 22.70±9.25 | −4.608 to 4.185 | 0.92 |
| SS (°) | | | | |
| Preoperative | 27.21±10.79 | 23.91±9.90 | −8.149 to 1.554 | 0.18 |
| Postoperative | 24.15±10.44 | 25.77±10.84 | −3.584 to 6.827 | 0.54 |
| PI (°) | 47.06±8.50 | 48.47±11.40 | −3.903 to 6.722 | 0.60 |
| Postoperative PI-LL (°) | 3.63±7.95 | 3.90 (−0.55, 12.65) | | 0.42 |
| PI-LL mismatch | 4/20 (25.0%) | 32/105 (30.5%) | | 0.31 |

Data are presented as mean ± standard deviation, median (interquartile range), or n (%). DIP, distal instrumentation-related problem; CI, confidence interval; LL, lumbar lordosis; LSL, lumbosacral lordosis; SVA, sagittal vertical axis; TPA, T1 pelvic angle; PT, pelvic tilt; SS, sacral slope; PI, pelvic incidence.

flexional moment of the distal uninstrumented level adjacent to the LIV. Therefore, for DLS patients who undergo long-instrumented spinal fusion, the effect of paraspinal muscle degeneration on the incidence of DIPs is more significant.

In the current study, significantly smaller rFCSA and higher MFI values of the MF, ES, and PSE were observed in patients with the development of DIPs. This finding was similar to the results of Yuan *et al.* (3) and Leng *et al.* (12), who reported the association between extensor muscle degeneration and instrumentation-related complications in patients with DLS. According to the literature, lean muscle mass could indirectly reflect muscle strength; therefore, the rFCSA was more sensitive than the rGCSA or MFI in predicting the prognosis of DLS patients (40,41). The results of the Delong test in the current study were consistent with those of previous studies. We found that the AUC of the rFCSA of the PSE was significantly greater than that of other MRI parameters, and this variable was identified as an independent predictive factor of DIPs by multivariable logistic regression analysis. There is no doubt

**Table 5** Multivariate logistic regression of the independent predictors of DIPs

| Variables | Odds ratio | 95% CI | | P value |
|---|---|---|---|---|
| | | Lower limit | Upper limit | |
| Preoperative PT | 0.942 | 0.867 | 1.022 | 0.15 |
| Postoperative LSL | 1.051 | 0.963 | 1.146 | 0.27 |
| Postoperative SVA | 1.047 | 1.003 | 1.093 | 0.04 |
| rFCSA of PSE | 0.958 | 0.936 | 0.981 | <0.001 |
| HU value of lumbosacral region | 0.941 | 0.906 | 0.977 | 0.002 |

DIPs, distal instrumentation-related problems; CI, confidence interval; PT, pelvic tilt; LSL, lumbosacral lordosis; SVA, sagittal vertical axis; rFCSA, relative functional cross-sectional area; PSE, paraspinal extensor muscle; HU, Hounsfield unit.

that posterior spine surgery causes PSE atrophy due to iatrogenic denervation, ischemia, and thermal damage (42). Therefore, patients with low preoperative muscularity are more susceptible to DIPs. For these patients, some strategies could be considered to reduce the risk. Multiple-rod constructs have been recommended to reduce the concentrated stress on the instrumentation of L5 or S1 (9). Avoiding extensive musculoligamentous dissection is also of paramount importance. As there was no significant association between the muscularity of the psoas and DIPs, a more minimally invasive lateral surgical approach combined with posterior percutaneous instrumentation could be performed to preserve the PSE at the distal level (43).

Spinopelvic fixation is another important protective procedure for decreasing the risk of distal failure in patients undergoing long spinal fusion surgery (13,25). Many cohort studies of patients undergoing spinopelvic fixation using S2-alar-iliac (S2AI) screws or iliac screws have been reported (44-48). However, in our hospital, the indications for spinopelvic fixation only include neuromuscular scoliosis, 3-CO at the lumbar spine, and revisions for lumbosacral failure. Most of the DLS patients in our hospital were elderly and had comorbidities (e.g., hypertension, chronic obstructive pulmonary disease, coronary artery disease, and diabetes mellitus). The spinal deformity severity in these patients was relatively mild (usually a Cobb angle <20° and an SVA <50 mm), mainly presenting as lateral spondylolisthesis, axial rotation, and anterior translation. The primary complaints of these patients were usually low back or leg pain rather than spinal deformity. To solve their problems with a lower risk of postoperative systemic complications and shorter time for surgery as well as anesthesia, we rarely perform radical 3-CO for these patients, and the UIV is commonly at the upper lumbar vertebra (L2) or lower thoracic region. Additionally, the performance of spinopelvic fixation may impact their HRQoL due to extensive dissection and sacroiliac joint violation (49,50). Therefore, spinopelvic fixation is not routinely performed for these patients. In the current study, none of the recruited patients had a history of spinal surgery, and only low-grade posterior column osteotomy (PCO) was performed. As a result, instrumentation was stopped at or above S1 for all recruited patients. The findings of this study may provide surgeons with an important caution that low preoperative paraspinal muscularity should also be an indication for spinopelvic fixation.

After the placement of instrumentation, additional compression loadings are exerted on the LIV. If the structural rigidity of the vertebra cannot adequately tolerate the alteration of compressive forces, bony failure occurs, leading to DIPs (17). Therefore, evaluation of vBMD is important before correction surgery for DLS. Although DXA scans are the gold standard for measuring BMD, they may not be reliable for evaluating cancellous bone in patients with spinal deformities, especially those with DLS (51). The HU value measured by CT scan continues to gain recognition because it could be a proxy for standard BMD and reflect bone strength (52,53). In the current study, the HU values of the lumbosacral region and LIV were significantly lower in patients with DIPs. The vertebra with a lower HU value usually had a lower Young's modulus, which indicated susceptibility to deformation when extra stress was exerted (54). The endplate of this vertebra may collapse, and the bone-screw interface could be loosened. The DeLong test showed that the HU values of the lumbosacral region had more predictive value than those of the LIV, indicating that surgeons should pay more attention to the deterioration of bone strength at the lower lumbar and lumbosacral junctions before surgery. The optimal cutoff value of this parameter was 112.03, which the maximizes sensitivity (93.3%) and specificity (80.0%) in predicting DIPs. These data are paramount to preoperative optimization for DLS patients to pursue satisfactory outcomes. For patients with suspiciously low HU values of the lumbosacral region, DXA is recommended to evaluate their standard BMD, and surgery should be postponed until after 3–6 months of anti-osteoporotic medication therapy, such as teriparatide. During surgery, bone cement-augmented screws could be applied to reinforce the lumbosacral region and minimize

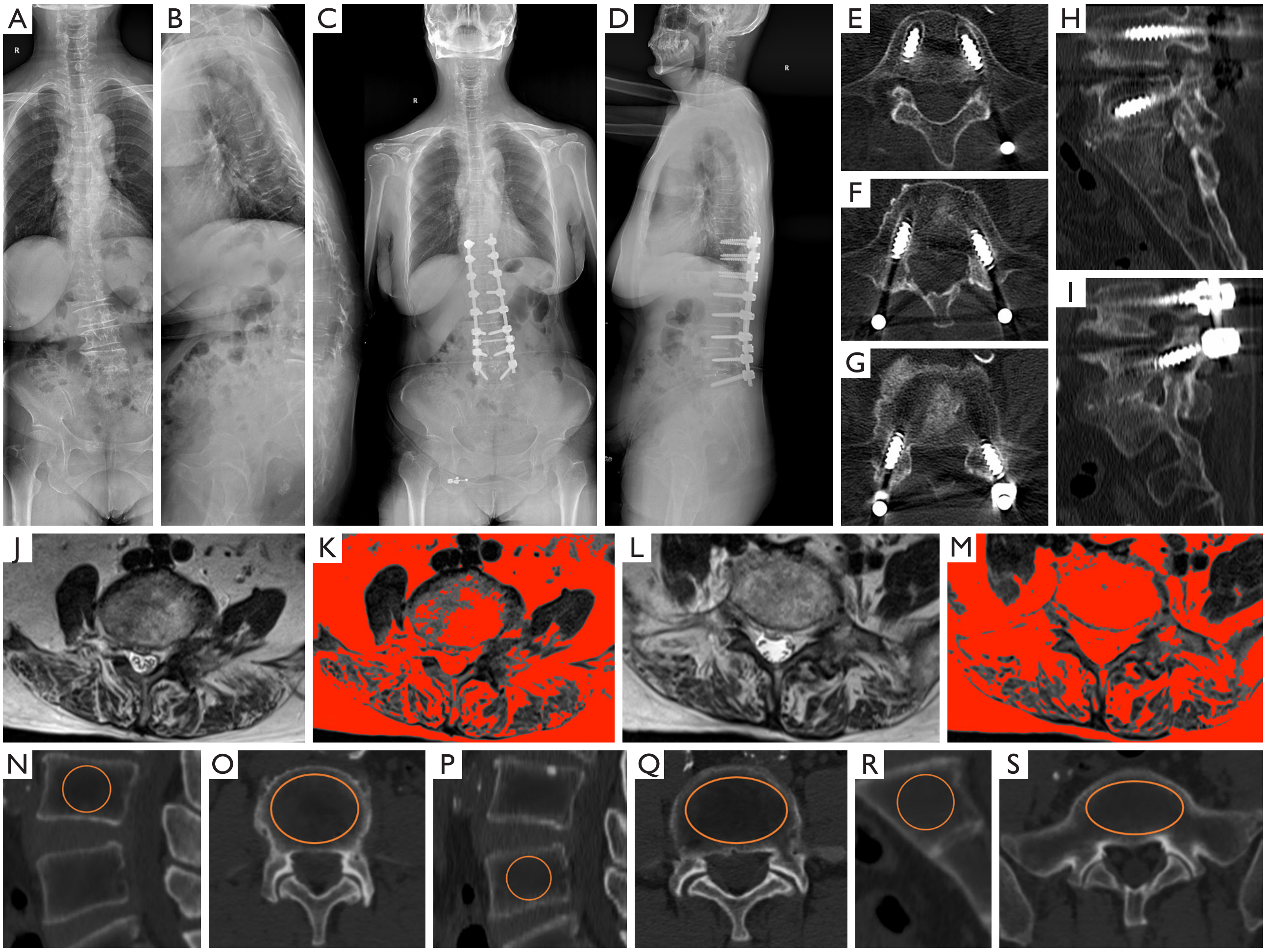


**Figure 7** An illustrative case. A 70-year-old female with degenerative lumbar scoliosis and kyphosis was admitted to the hospital due to low back pain, leg pain, and intermittent claudication. She underwent long-instrumented spinal fusion from T10-L5, and she began antiosteoporosis therapy after discharge from the hospital. Two years after surgery, this patient complained of recurrent severe low back pain. The lumbar spine CT scan showed pedicle screw loosening at the LIV. The preoperative lumbar spine MRI showed low muscularity of the paraspinal muscle. The rFCSA for the PSE was 137.40. The preoperative lumbar spine CT scan showed low bone mass of the vertebra. The HU values of the lumbosacral region and LIV were 96.23 and 90.01, respectively. (A-D) Preoperative and two-year postoperative standing full-length spine radiographs; (E-I) two-year postoperative lumbar spine CT scan of the LIV; (J-M) measurement of the paraspinal muscle using preoperative lumbar spinal MRI at L4 and L5; (N-S) measurement of the HU values of the lumbosacral region and LIV using preoperative lumbar spine CT scans at L4, L5, and S1. The orange circles indicate the region of interest. CT, computed tomography; LIV, lower instrumented vertebra; MRI, magnetic resonance imaging; rFCSA, relative functional cross-sectional area; PSE, paraspinal extensor muscle; HU, Hounsfield unit.

the risk of DIPs (55). For patients with instrumentation ending at S1, L5-S1 anterior column support should also be considered, which could enhance the stability of the lumbosacral junction and decrease the mechanical complication rate in this region (56).

Biomechanical studies revealed that an anterior shift of the gravity center relative to the LIV can cause additional loadings and stress on the endplate and instrumentation, increasing the risk of instrumentation failure (57,58). Additionally, it has been reported that paraspinal muscularity in the lower lumbar spine can only maintain local alignment rather than global balance (20). Consistent with previous studies, the current study revealed that a larger postoperative SVA was an independent predictive factor of DIPs. For elderly patients with DLS, the flexibility of the spine is always rigid and has limited compensatory ability for postoperative sagittal malalignment. Radical posterior 3-CO, such as pedicle subtraction osteotomy (PSO), is usually needed to better restore the SVA during surgery. However, applying high-grade posterior osteotomy is also a risk factor for mechanical complications (59). Therefore, the anterior column realignment (ACR) procedure could be considered an alternative, performed through an anterior or lateral approach with no requirement for paraspinal muscle dissection (60). For DLS patients with severe preoperative sagittal imbalance, ACR combined with only PCO was adequate to restore sagittal alignment, which was as effective as PSO.

### *Limitations*

Several limitations should be noted in this study. First, muscularity was only evaluated by CSA or MFI values measured by MRI, while ultrasound shear-wave elastography may be a better tool to directly assess paraspinal muscle function (61). Second, muscle strength and daily activities, which are important components in spinal mechanics, were not assessed in this study according to the guidance from the Asian Working Group for Sarcopenia (62). Third, posterior spine surgery commonly injures the paraspinal muscle; however, postoperative lumbar MRI is not routinely performed to evaluate the association between DIPs and the paraspinal muscle in postoperative variations. Last, the sample size was still limited, and the duration of follow-up was not long enough, which may hinder this study from detecting other risk factors.

## Conclusions

The incidence of DIPs in patients who underwent long-instrumented spinal fusion for DLS was 16.0%. Lower muscularity of the PSE and vBMD of the lumbosacral region were independent predictive factors of the development of DIPs. Higher postoperative SVA values were also independently associated with this complication. Surgeons should pay attention to the preoperative evaluation of the paraspinal muscle and bone mass for patients with DLS, and targeted perioperative strategies should be considered.

## Acknowledgments

*Funding:* None.

## Footnote

*Reporting Checklist:* The authors have completed the STROBE reporting checklist. Available at https://qims.amegroups.com/article/view/10.21037/qims-22-1394/rc

*Conflicts of Interest:* All authors have completed the ICMJE uniform disclosure form (available at https://qims.amegroups.com/article/view/10.21037/qims-22-1394/coif). The authors have no conflicts of interest to declare.

*Ethical Statement:* The authors are accountable for all aspects of the work by ensuring that questions related to the accuracy or integrity of any part of the work are appropriately investigated and resolved. The study was conducted in accordance with the Declaration of Helsinki (as revised in 2013). The study was approved by the Research Ethics Committee of Beijing Chao-Yang Hospital (No. 2021-09-07-10), and the need for individual consent for this retrospective analysis was waived.



## References

1. Wong E, Altaf F, Oh LJ, Gray RJ. Adult Degenerative Lumbar Scoliosis. Orthopedics 2017;40:e930-9.
2. Zhan X, Zhan X, Yu J, Moore G, Li F, Xi X, Zeng Z, Yin S, Yu Y, Cheng L. Correlation between direction of pedicle screw and restoration of lumbar degenerative scoliosis in degenerative lumbar spondylolisthesis: a retrospective study. Quant Imaging Med Surg 2023;13:1740-52.
3. Yuan L, Zeng Y, Chen Z, Li W, Zhang X, Mai S. Degenerative lumbar scoliosis patients with proximal junctional kyphosis have lower muscularity,

fatty degeneration at the lumbar area. Eur Spine J 2021;30:1133-43.
4. Ferrero E, Khalifé M, Marie-Hardy L, Regnard N, Feydy A, De Loubresse CG, Zakine S, Guigui P. Do Curve Characteristics Influence Stenosis Location and Occurrence of Radicular Pain in Adult Degenerative Scoliosis? Spine Deform 2019;7:472-80.
5. Hong JY, Suh SW, Modi HN, Hur CY, Song HR, Park JH. The prevalence and radiological findings in 1347 elderly patients with scoliosis. J Bone Joint Surg Br 2010;92:980-3.
6. Kebaish KM, Neubauer PR, Voros GD, Khoshnevisan MA, Skolasky RL. Scoliosis in adults aged forty years and older: prevalence and relationship to age, race, and gender. Spine (Phila Pa 1976) 2011;36:731-6.
7. Xu L, Sun X, Huang S, Zhu Z, Qiao J, Zhu F, Mao S, Ding Y, Qiu Y. Degenerative lumbar scoliosis in Chinese Han population: prevalence and relationship to age, gender, bone mineral density, and body mass index. Eur Spine J 2013;22:1326-31.
8. Yuan L, Zhang X, Zeng Y, Chen Z, Li W. Incidence, Risk, and Outcome of Pedicle Screw Loosening in Degenerative Lumbar Scoliosis Patients Undergoing Long-Segment Fusion. Global Spine J 2021. [Epub ahead of print]. doi: 10.1177/21925682211017477.
9. Lamas V, Charles YP, Tuzin N, Steib JP. Comparison of degenerative lumbar scoliosis correction and risk for mechanical failure using posterior 2-rod instrumentation versus 4-rod instrumentation and interbody fusion. Eur Spine J 2021;30:1965-77.
10. Sebaaly A, Gehrchen M, Silvestre C, Kharrat K, Bari TJ, Kreichati G, Rizkallah M, Roussouly P. Mechanical complications in adult spinal deformity and the effect of restoring the spinal shapes according to the Roussouly classification: a multicentric study. Eur Spine J 2020;29:904-13.
11. Zhang H, Hai Y, Meng X, Zhang X, Jiang T, Xu G, Zou C, Xing Y. Validity of the Roussouly classification system for assessing distal junctional problems after long instrumented spinal fusion in degenerative scoliosis. Eur Spine J 2022;31:258-66.
12. Leng J, Han G, Zeng Y, Chen Z, Li W. The Effect of Paraspinal Muscle Degeneration on Distal Pedicle Screw Loosening Following Corrective Surgery for Degenerative Lumbar Scoliosis. Spine (Phila Pa 1976) 2020;45:590-8.
13. Yasuda T, Hasegawa T, Yamato Y, Kobayashi S, Togawa D, Banno T, Arima H, Oe S, Matsuyama Y. Lumbosacral Junctional Failures After Long Spinal Fusion for Adult Spinal Deformity-Which Vertebra Is the Preferred Distal Instrumented Vertebra? Spine Deform 2016;4:378-84.
14. Mattei TA, Fassett DR. Combined S-1 and S-2 sacral alar-iliac screws as a salvage technique for pelvic fixation after pseudarthrosis and lumbosacropelvic instability: technical note. J Neurosurg Spine 2013;19:321-30.
15. Núñez-Pereira S, Pellisé F, Vila-Casademunt A, Alanay A, Acaraglou E, Obeid I, Sánchez Pérez-Grueso FJ, Kleinstück F; . Impact of resolved early major complications on 2-year follow-up outcome following adult spinal deformity surgery. Eur Spine J 2019;28:2208-15.
16. Arlet V, Aebi M. Junctional spinal disorders in operated adult spinal deformities: present understanding and future perspectives. Eur Spine J 2013;22 Suppl 2:S276-95.
17. St Jeor JD, Jackson TJ, Xiong AE, Freedman BA, Sebastian AS, Currier BL, Fogelson JL, Bydon M, Nassr A, Elder BD. Average Lumbar Hounsfield Units Predicts Osteoporosis-Related Complications Following Lumbar Spine Fusion. Global Spine J 2022;12:851-7.
18. Bae J, Sathe A, Lee SM, Theologis AA, Deviren V, Lee SH. Correlation of Paraspinal Muscle Mass With Decompensation of Sagittal Adult Spinal Deformity After Setting of Fatigue Post 10-Minute Walk. Neurospine 2021;18:495-503.
19. Xie D, Zhang J, Ding W, Yang S, Yang D, Ma L, Zhang J. Abnormal change of paravertebral muscle in adult degenerative scoliosis and its association with bony structural parameters. Eur Spine J 2019;28:1626-37.
20. Han G, Wang W, Zhou S, Li W, Zhang B, Sun Z, Li W. Paraspinal Muscle Degeneration as an Independent Risk for Loss of Local Alignment in Degenerative Lumbar Scoliosis Patients After Corrective Surgery. Global Spine J 2021. [Epub ahead of print]. doi: 10.1177/21925682211022284.
21. Duan PG, Mummaneni PV, Rivera J, Guinn JMV, Wang M, Xi Z, Li B, Wu HH, Ames CP, Burch S, Berven SH, Chou D. The association between lower Hounsfield units of the upper instrumented vertebra and proximal junctional kyphosis in adult spinal deformity surgery with a minimum 2-year follow-up. Neurosurg Focus 2020;49:E7.
22. Pennington Z, Cottrill E, Ahmed AK, Passias P, Protopsaltis T, Neuman B, Kebaish KM, Ehresman J, Westbroek EM, Goodwin ML, Sciubba DM. Paraspinal muscle size as an independent risk factor for proximal junctional kyphosis in patients undergoing thoracolumbar fusion. J Neurosurg Spine 2019;31:380-8.
23. Goubert D, De Pauw R, Meeus M, Willems T, Cagnie B, Schouppe S, Van Oosterwijck J, Dhondt E, Danneels L.

Lumbar muscle structure and function in chronic versus recurrent low back pain: a cross-sectional study. Spine J 2017;17:1285-96.
24. Xu F, Zou D, Li W, Sun Z, Jiang S, Zhou S, Li Z. Hounsfield units of the vertebral body and pedicle as predictors of pedicle screw loosening after degenerative lumbar spine surgery. Neurosurg Focus 2020;49:E10.
25. McDonnell JM, Evans SR, Ahern DP, Cunniffe G, Kepler C, Vaccaro A, Kaye ID, Morrissey PB, Wagner SC, Sebastian A, Butler JS. Risk factors for distal junctional failure in long-construct instrumentation for adult spinal deformity. Eur Spine J 2022;31:3654-61.
26. Hyun SJ, Kim YJ, Rhim SC. Patients with proximal junctional kyphosis after stopping at thoracolumbar junction have lower muscularity, fatty degeneration at the thoracolumbar area. Spine J 2016;16:1095-101.
27. Zou D, Li W, Xu F, Du G. Use of Hounsfield units of S1 body to diagnose osteoporosis in patients with lumbar degenerative diseases. Neurosurg Focus 2019;46:E6.
28. Lee CH, Chung CK, Sohn MJ, Kim CH. Short Limited Fusion Versus Long Fusion With Deformity Correction for Spinal Stenosis With Balanced De Novo Degenerative Lumbar Scoliosis: A Meta-analysis of Direct Comparative Studies. Spine (Phila Pa 1976) 2017;42:E1126-32.
29. Li Y, Ou Y, Zhu Y, He B, Xu S, Yu H. Effectiveness of Short-Segment Fixation versus Long-Segment Fixation for Degenerative Scoliosis with Cobb Angle 20°~40°: A Retrospective Observational Study. Med Sci Monit 2020;26:e923656.
30. Zhang HC, Yu HL, Yang HF, Sun PF, Wu HT, Zhan Y, Wang Z, Xiang LB. Short-segment decompression/fusion versus long-segment decompression/fusion and osteotomy for Lenke-Silva type VI adult degenerative scoliosis. Chin Med J (Engl) 2019;132:2543-9.
31. Anand N, Agrawal A, Ravinsky R, Khanderhoo B, Kahwaty S, Chung A. The prevalence of proximal junctional kyphosis (PJK) and proximal junctional failure (PJF) in patients undergoing circumferential minimally invasive surgical (cMIS) correction for adult spinal deformity: long-term 2- to 13-year follow-up. Spine Deform 2021;9:1433-41.
32. Doodkorte RJP, Vercoulen TFG, Roth AK, de Bie RA, Willems PC. Instrumentation techniques to prevent proximal junctional kyphosis and proximal junctional failure in adult spinal deformity correction-a systematic review of biomechanical studies. Spine J 2021;21:842-54.
33. Hyun SJ, Lee BH, Park JH, Kim KJ, Jahng TA, Kim HJ. Proximal Junctional Kyphosis and Proximal Junctional Failure Following Adult Spinal Deformity Surgery. Korean J Spine 2017;14:126-32.
34. Mikula AL, Lakomkin N, Pennington Z, Pinter ZW, Nassr A, Freedman B, Sebastian AS, Abode-Iyamah K, Bydon M, Ames CP, Fogelson JL, Elder BD. Association between lower Hounsfield units and proximal junctional kyphosis and failure at the upper thoracic spine. J Neurosurg Spine 2022. [Epub ahead of print]. doi: 10.3171/2022.3.SPINE22197.
35. Arima H, Hasegawa T, Yamato Y, Yoshida G, Banno T, Oe S, Mihara Y, Ide K, Watanabe Y, Nakai K, Kurosu K, Matsuyama Y. Clinical Outcomes and Complications of Corrective Fusion Surgery Down to L4, L5, and the Pelvis for Adult Scoliosis in Patients Younger than 50 Years. Spine Surg Relat Res 2022;6:518-25.
36. Katsu M, Ohba T, Ebata S, Oba H, Koyama K, Haro H. Potential Role of Paraspinal Musculature in the Maintenance of Spinopelvic Alignment in Patients With Adult Spinal Deformities. Clin Spine Surg 2020;33:E76-80.
37. Pan A, Yang H, Hai Y, Liu Y, Zhang X, Ding H, Li Y, Lu H, Ding Z, Xu Y, Pei B. Adding sacral anchors through an S1 alar screw and multirod construct as a strategy for lumbosacral junction augmentation: an in vitro comparison to S1 pedicle screws alone with sacroiliac fixation. J Neurosurg Spine 2022;38:107-14.
38. Kim JH, Horton W, Hamasaki T, Freedman B, Whitesides TE Jr, Hutton WC. Spinal instrumentation for sacral-pelvic fixation: a biomechanical comparison between constructs ending with either S2 bicortical, bitriangulated screws or iliac screws. J Spinal Disord Tech 2010;23:506-12.
39. Kang S, Chang MC, Kim H, Kim J, Jang Y, Park D, Hwang JM. The Effects of Paraspinal Muscle Volume on Physiological Load on the Lumbar Vertebral Column: A Finite-Element Study. Spine (Phila Pa 1976) 2021;46:E1015-21.
40. Chen L, Nelson DR, Zhao Y, Cui Z, Johnston JA. Relationship between muscle mass and muscle strength, and the impact of comorbidities: a population-based, cross-sectional study of older adults in the United States. BMC Geriatr 2013;13:74.
41. Fortin M, Wilk N, Dobrescu O, Martel P, Santaguida C, Weber MH. Relationship between cervical muscle morphology evaluated by MRI, cervical muscle strength and functional outcomes in patients with degenerative cervical myelopathy. Musculoskelet Sci Pract 2018;38:1-7.
42. Pourtaheri S, Issa K, Lord E, Ajiboye R, Drysch A, Hwang K, Faloon M, Sinha K, Emami A. Paraspinal

 

Muscle Atrophy After Lumbar Spine Surgery. Orthopedics 2016;39:e209-14.
43. Yang H, Liu J, Hai Y, Han B. What Are the Benefits of Lateral Lumbar Interbody Fusion on the Treatment of Adult Spinal Deformity: A Systematic Review and Meta-Analysis Deformity. Global Spine J 2023;13:172-87.
44. Lee NJ, Marciano G, Puvanesarajah V, Park PJ, Clifton WE, Kwan K, Morrissette CR, Williams JL, Fields M, Hassan FM, Angevine PD, Mandigo CE, Lombardi JM, Sardar ZM, Lehman RA, Lenke LG. Incidence, mechanism, and protective strategies for 2-year pelvic fixation failure after adult spinal deformity surgery with a minimum six-level fusion. J Neurosurg Spine 2022;38:208-16.
45. Lee NJ, Park PJ, Puvanesarajah V, Clifton WE, Kwan K, Morrissette CR, Williams JL, Fields MW, Leung E, Hassan FM, Angevine PD, Mandigo CE, Lombardi JM, Sardar ZM, Lehman RA, Lenke LG. How common is acute pelvic fixation failure after adult spine surgery? A single-center study of 358 patients. J Neurosurg Spine 2022;38:91-7.
46. Lertudomphonwanit T, Bridwell KH, Kelly MP, Punyarat P, Theologis A, Sides BA, Gupta MC. Relationship of the character of rod fractures on outcomes following long thoracolumbar fusion to the sacrum for adult spinal deformity. Spine J 2020;20:1452-63.
47. Martin CT, Polly DW, Holton KJ, San Miguel-Ruiz JE, Albersheim M, Lender P, Sembrano JN, Hunt MA, Jones KE. Acute failure of S2-alar-iliac screw pelvic fixation in adult spinal deformity: novel failure mechanism, case series, and review of the literature. J Neurosurg Spine 2021;36:53-61.
48. Sardi JP, Lazaro B, Smith JS, Kelly MP, Dial B, Hills J, Yanik EL, Gupta M, Baldus CR, Yen CP, Lafage V, Ames CP, Bess S, Schwab F, Shaffrey CI, Bridwell KH. Rod fractures in thoracolumbar fusions to the sacrum/pelvis for adult symptomatic lumbar scoliosis: long-term follow-up of a prospective, multicenter cohort of 160 patients. J Neurosurg Spine 2022;38:217-29.
49. Gao Z, Sun X, Chen C, Teng Z, Xu B, Ma X, Wang Z, Yang Q. Comparative radiological outcomes and complications of sacral-2-alar iliac screw versus iliac screw for sacropelvic fixation. Eur Spine J 2021;30:2257-70.
50. Kozaki T, Hashizume H, Nishiyama D, Iwasaki H, Tsutsui S, Takami M, Yukawa Y, Minamide A, Taniguchi T, Nagata K, Fukui D, Tamai H, Taiji R, Murata S, Oka H, Yamada H. Adjacent segment disease on hip joint as a complication of spinal fusion surgery including sacroiliac joint fixation. Eur Spine J 2021;30:1314-9.
51. Wang H, Zou D, Sun Z, Wang L, Ding W, Li W. Hounsfield Unit for Assessing Vertebral Bone Quality and Asymmetrical Vertebral Degeneration in Degenerative Lumbar Scoliosis. Spine (Phila Pa 1976) 2020;45:1559-66.
52. Cheng Y, Yang H, Hai Y, Pan A, Zhang Y, Zhou L. Hounsfield unit for assessing asymmetrical loss of vertebral bone mineral density and its correlation with curve severity in adolescent idiopathic scoliosis. Front Surg 2022;9:1000031.
53. Zaidi Q, Danisa OA, Cheng W. Measurement Techniques and Utility of Hounsfield Unit Values for Assessment of Bone Quality Prior to Spinal Instrumentation: A Review of Current Literature. Spine (Phila Pa 1976) 2019;44:E239-44.
54. Ogurkowska MB, Błaszczyk A. Distribution of Young's modulus at various sampling points in a human lumbar spine vertebral body. Spine J 2020;20:1861-75.
55. Singh V, Mahajan R, Das K, Chhabra HS, Rustagi T. Surgical Trend Analysis for Use of Cement Augmented Pedicle Screws in Osteoporosis of Spine: A Systematic Review (2000-2017). Global Spine J 2019;9:783-95.
56. Dinizo M, Srisanguan K, Dolgalev I, Errico TJ, Raman T. Pseudarthrosis and Rod Fracture Rates After Transforaminal Lumbar Interbody Fusion at the Caudal Levels of Long Constructs for Adult Spinal Deformity Surgery. World Neurosurg 2021;155:e605-11.
57. Cho W, Wang W, Bucklen B. The role of sagittal alignment in predicting major failure of lumbopelvic instrumentation: a biomechanical validation of lumbopelvic failure classification. Spine Deform 2020;8:561-8.
58. Cho W, Wang W, Bucklen B, De la Garza Ramos R, Yassari R. The Role of Biological Fusion and Anterior Column Support in a Long Lumbopelvic Spinal Fixation and Its Effect on the S1 Screw-An In Silico Biomechanics Analysis. Spine (Phila Pa 1976) 2021;46:E250-6.
59. Charosky S, Guigui P, Blamoutier A, Roussouly P, Chopin D; . Complications and risk factors of primary adult scoliosis surgery: a multicenter study of 306 patients. Spine (Phila Pa 1976) 2012;37:693-700.
60. Mundis GM Jr, Turner JD, Kabirian N, Pawelek J, Eastlack RK, Uribe J, Klineberg E, Bess S, Ames C, Deviren V, Nguyen S, Lafage V, Akbarnia BA; . Anterior Column Realignment has Similar Results to Pedicle Subtraction Osteotomy in Treating Adults with Sagittal Plane Deformity. World Neurosurg 2017;105:249-56.
61. Alis D, Durmaz ESM, Alis C, Erol BC, Okur B, Kizilkilic O, Mihmanli I. Shear Wave Elastography of the Lumbar

Multifidus Muscle in Patients With Unilateral Lumbar Disk Herniation. J Ultrasound Med 2019;38:1695-703.
62. Chen LK, Woo J, Assantachai P, Auyeung TW, Chou MY, Iijima K, et al. Asian Working Group for Sarcopenia: 2019 Consensus Update on Sarcopenia Diagnosis and Treatment. J Am Med Dir Assoc 2020;21:300-307.e2.

**Cite this article as:** Yang H, Li Z, Hai Y, Zhang H. The role of lumbosacral paraspinal muscle degeneration and low vertebral bone mineral density on distal instrumentation-related problems following long-instrumented spinal fusion for degenerative lumbar scoliosis: a retrospective cohort study. Quant Imaging Med Surg 2023;13(7):4475-4492. doi: 10.21037/qims-22-1394

 